

Supporting Information

Electrostatically-Driven Guanidinium Interaction Domains that Control Hydrogel-Mediated Protein Delivery In Vivo.

Stephen E. Miller,[†] Yuji Yamada,[†] Nimit Patel,^{||} Ernesto Suárez,⁺ Caroline Andrews,[‡] Steven Tau,[†] Brian T. Luke,⁺ Raul E. Cachau,⁺ and Joel P. Schneider^{†*}

National Cancer Institute, Frederick, MD 21702 United States: [†]Chemical Biology Laboratory; [‡]Cancer and Inflammation Program

Frederick National Laboratory for Cancer Research, Frederick, MD 21702, United States: ^{||}Small Animal Imaging Program; ⁺Advanced Biomedical Computational Science Group

Supporting Methods-----	2
General -----	2
Peptide Synthesis and Purification-----	2
Plasmid Generation for ID-Containing Proteins-----	3
Expression and Purification of Proteins-----	3
UV and Fluorescence Measurements -----	6
In Vitro Gel Release Experiments-----	6
HL116 Cell Activity Assays-----	7
Oscillatory Rheology-----	8
Circular Dichroism-----	8
Transmission Electron Microscopy-----	8
In Vivo Gel Release Experiments -----	9
Histological Analysis of Injection Site Tissue-----	9
Modelling the AcVES3 fiber/ID interaction -----	10
Figure S1. Sequences and SDS-PAGE gels for fluorescent proteins used in this study.-----	13
Figure S2. Synthesis of AcVES3 by solid phase peptide synthesis.-----	14
Figure S3. Analytical HPLC for AcVES3 and D-AcVES3, with tabulated mass spec data.-----	15
Figure S4. Structural analysis of AcVES3 -----	16
Figure S5. Rheology of empty and protein loaded hydrogels. -----	17
Figure S6. Effect of high salt content on the release of ID5-EGFP. -----	18
Figure S7. Normalized absorbance and fluorescence spectra for EGFP analogs. -----	18
Figure S8. Images of EGFP loaded hydrogels at selected time points.-----	19
Figure S9. Encapsulating EGFP into positively charged hydrogels formed from cationic self-assembling peptides. -----	19
Figure S10. Image of co-encapsulated EGFP and ID5-mRuby3 in AcVES3 hydrogel. -----	19
Figure S11. Sequences and SDS-PAGE gels for IFN α 5 and its ID analogs.-----	20
Figure S12. CD spectra of IFN α 5 analogs.-----	21
Figure S13. Model of the AcVES3 fiber used for MD simulations. -----	21
Figure S14. Assessing the preferred binding geometry of ID6. -----	22
Figure S15. In vitro analysis of mRuby3 and ID5-mRuby3 release from AcVES3 hydrogels. -----	23
Figure S16. In vivo fluorescent images for mRuby3/ID5-mRuby3 release from AcVES3 hydrogels at selected time points. -----	24
Table S1. Parameters used in molecular dynamics simulations.-----	25
Supporting References -----	25

Supporting Methods

General

No unexpected or unusually high safety hazards were encountered during the course of this work.

All reagents and kits were purchased from commercial vendors. The initial EGFP and mRuby3 template plasmids, as well as the pDonr253 and pDest527 vectors, were obtained from the Protein Expression Laboratory of the Frederick National Laboratory for Cancer Research. The initial pPAL7-IFN α vector and the HL116 cells were obtained from Dr. Mark Walter. Experiments utilizing kits or the transformation of vectors into competent cells were performed following the protocols from their respective manufacturers, which are noted below for each. HEPES buffered saline (HBS) was used for all hydrogel experiments with 1X HBS = 25 mM HEPES, 150 mM NaCl, pH 7.4. LC buffers consisted of 20 mM NH₄HCO₃ (Std C) and 20 mM NH₄HCO₃ in 80% acetonitrile (Std D). Calculated protein molecular weights and isoelectric points were determined using EXPASY ProtParam. NuPAGE 4-12% Bis-Tris gels and SeeBlue Plus2 prestained standard (both Invitrogen) were used for protein analysis.

Peptide Synthesis and Purification

AcVES3 was synthesized on ProTide resin (0.56 mmol/g) using a CEM Liberty Blue microwave-assisted peptide synthesizer (Figure S2). Fmoc deprotection was performed using 20% piperidine in DMF at 90 °C for 1 min. The first 11 couplings were performed using 5 eq of amino acid/DIC/Oxyma in DMF at 90 °C for 4 min. For the valine residue immediately following the D-proline, room temperature triple coupling was performed using 5 eq of amino acid/HCTU/DIEA in DMF (30 min for each coupling). The subsequent glutamic acid and valine residues were double coupled using room temperature HCTU/DIEA conditions. The last 6 residues were added using the DIC/Oxyma conditions. After capping the N-terminus with 10% acetic anhydride in DMF, the peptide was cleaved from resin using 95% TFA, 2.5 % TIPS, and 2.5% H₂O for 3 hr. The resin was then filtered and the collected filtrate was concentrated by a stream of argon. Following ether precipitation, the crude solid was dried under vacuum overnight, then resuspended in Milli-Q water, frozen and lyophilized. AcVES3 was purified by prep-HPLC. The crude peptide was dissolved at 3 mg/mL in Std C by rocking at RT for over an hour, with intermittent vortexing for 30 s at a time. Per run, 5 mL of syringe filtered sample was injected into a Waters 600 system, equipped with a Waters 2489 UV Detector and a Phenomenex PolymerX RP-1 column (250 x 21.2 mm, 10 μ m, heated to 40 °C). A gradient of 1% Std D per min was used for 25 min, followed by 0.5 % Std D per min for 150 min. The UV trace at 220 nm was monitored and fractions containing the major peptide peak were combined and lyophilized. Purity was assessed by LCMS (Shimadzu LCMS 2020) and analytical HPLC (Agilent 1200 series, PolymerX RP-1 column, 250 x 4.6 mm, 10 μ m) using gradients of 1% Std D per min. Purified AcVES3 was dissolved at 1 mg/mL in Std C and converted to the sodium salt by adding 1 eq NaOH per glutamate residue (5 eq NaOH per 1 eq peptide) using a 0.1 M NaOH stock. The solution was then frozen and lyophilized to afford a white powder. An analogous procedure was used in the synthesis/purification of D-AcVES3 (note: the HCTU/DIEA triple or double coupling steps mentioned above were done for the three residues following the L-proline in D-AcVES3).

Plasmid Generation for ID-Containing Proteins

Generation of EGFP/mRuby3 analogs: Primers (IDT) encoding genes of interest, including N-terminal cleavage sites for His-tag removal (FXa or TEV), underwent overlap-extension PCR using the Qiagen Fast Cycling PCR kit with either an EGFP or mRuby3 containing plasmid as the template. PCR products were purified using the QIAquick PCR purification kit, then subjected to Gateway BP cloning (Invitrogen) using the pDonr253 donor vector, transformed into DH5 α subcloning efficiency cells (Invitrogen), and plated on LB agar plates containing 50 μ g/mL spectinomycin. The plates were grown overnight at 37 °C. Single colonies were picked and grown overnight in 10 mL LB media with 50 μ g/mL spectinomycin at 37 °C, 250 RPM. Minipreps (Qiagen) were performed to isolate amplified entry vectors. Once the sequences were validated (using Macrogen standard sequencing), the vectors were subjected to Gateway LR cloning (Invitrogen) using the pDest527 vector, transformed into DH5 α subcloning efficiency cells, and plated on LB agar plates containing 100 μ g/mL ampicillin. The plates were grown overnight at 37 °C. Single colonies were picked and grown overnight in 10 mL LB media with 100 μ g/mL ampicillin at 37 °C, 250 RPM. Minipreps were performed to isolate amplified expression vectors and the sequences were validated prior to expression. When not in use, vectors were stored at -20 C.

Generation of IFN α 5 analogs: Linearization of the pPAL7-IFN α 5 gene was performed by PCR (Qiagen Fast Cycling PCR Kit), utilizing primers that introduced linker-ID5 overhang genes at the 3' end of IFN α 5 and the 5' end of the stop codon. The PCR product was then subjected to the HiFi DNA assembly protocol (NEB) with a double stranded gene encoding linker-ID5 to generate the expression vector. The crude vector was transformed into NEB5 α cells and plated onto LB agar plates containing 100 μ g/mL carbenicillin. The plates were grown overnight at 37 °C. Single colonies were picked and grown overnight in 10 mL LB media containing 100 μ g/mL carbenicillin. Minipreps were performed to isolate amplified expression vector and the sequence was validated prior to expression. To create the ID3-containing vector, primers were used with the Quikchange Lightning kit (Agilent) to insert two stop codons within the ID region of IFN α 5-ID5 vector to create the truncated ID3. After DpnI treatment, the Quikchange reaction solution was transformed into XL10-Gold cells and plated onto LB agar plates containing 100 μ g/mL carbenicillin. The plates were grown overnight at 37 °C. Single colonies were picked and grown overnight in 10 mL LB media containing 100 μ g/mL carbenicillin. Minipreps were performed to isolate amplified expression vector and the sequence was validated prior to expression. When not in use, vectors were stored at -20 C.

Expression and Purification of Proteins

Expression of EGFP/mRuby3 analogs: Expression vectors were transformed into Rosetta 2 DE3 pLyss competent cells (Millipore) and plated on LB Agar containing 100 μ g/mL carbenicillin and 34 μ g/mL chloramphenicol. The plates were grown overnight at 37 °C. Single colonies were picked and grown overnight in 20 mL LB media (100 μ g/mL carbenicillin, 34 μ g/mL chloramphenicol) at 37 °C, 250 RPM. 5 mL of overnight culture was used to seed 500 mL of LB (100 μ g/mL carbenicillin, 34 μ g/mL chloramphenicol), and the culture was shaken at 37 °C, 250 RPM. OD600 was monitored until reaching a value of 0.6-0.8, usually around 2-2.5 hr. At this point, the incubator temperature was reduced to 17 °C and the flasks were cooled for 15 min. To induce expression, IPTG was added to a final concentration of 0.5 mM and the flasks were shaken at 17 °C, 250 RPM for 20 h. Each flask was split into 2 x 250 mL centrifuge bottles and spun down

for 20 min at 7000 g and 4 °C. The supernatant was removed, and the pellets were stored at -80 °C until purification.

Purification of EGFP/mRuby3 analogs: Pellets (from ~250 mL culture) were resuspended in 20 mL lysis buffer (50 mM sodium phosphate pH 8.0, 100 mM NaCl, 10 mM imidazole, 1x Bug Buster, and 1 EDTA-free protease inhibitor tablet), placed on ice, and subjected to sonication (25 % amp, 1 s on, 1 s off, 1.5 min total on). The lysate was then centrifuged at 4 °C, 7000 g for 20 min and the supernatant was syringe filtered (0.45 μ m). Using a GE P-960 sample pump, the lysate was injected into a GE ATKA FPLC system equipped with a 5mL Talon resin column. Purification was carried out using a step gradient of 0/20/60/100 % B (Buffer A: 50 mM sodium phosphate pH 8.0, 100 mM NaCl, 10 mM imidazole; Buffer B: 50 mM sodium phosphate pH 8.0, 100 mM NaCl, 100 mM imidazole). Fractions were monitored for absorbance at 280/488 nm (EGFP) or 280/558 nm (mRuby3), typically eluting at 60 and/or 100% B. Purity was confirmed by SDS PAGE gel, with the pure fractions combined and subjected to several rounds of buffer exchanges into 50 mM sodium phosphate pH 8.0, 100 mM NaCl using Amicon Ultra-15 centrifugal filters (MWCO 10 kDa) to achieve sub-micromolar imidazole concentrations. The concentrated protein was diluted to 1.5 mL, and the concentration was determined by UV (EGFP: ϵ = 56,000 M⁻¹ cm⁻¹ at 488 nm; mRuby3: ϵ = 128,000 M⁻¹ cm⁻¹ at 558 nm). Typical yields were 20-60 mg per L culture.

Removal of NH6 domain for EGFP/mRuby3 analogs: For removal of the N-terminal His-6 tag encoded in the pDest527 expression vector, FXa or TEV proteases were employed. For the generation free EGFP or mRuby3, FXa cleavage was used. A typical experiment would use 5 mg (determined by UV) of NH6-FXa-EGFP/mRuby3 in 20 mL of cleavage buffer (20 mM Tris, pH 8.0, 100 mM NaCl, 2 mM CaCl₂) and 100 μ g of FXa (protein:enzyme weight ratio of ~ 50:1). The reaction was monitored by SDS PAGE gel and was typically completed within 7 hr. The reaction solution was added to prewashed p-aminobenzamidine functionalized resin to bind FXa, allowed to rock at RT for 30 min, and then the resin was filtered using an empty polypropylene column. EGFP/mRuby3 was exchanged in to Milli-Q water using Amicon Ultra-15 filters (MWCO 10 kDa) and typically achieved near quantitative yields (~4.5 mg from 5 mg NH6 fusion). The unstructured nature of the IDs made them susceptible to non-specific cleavage by FXa, and a TEV cleavage site was installed to circumvent this. The protocol for cleavage by Halo-TEV protease (Promega) followed that of the manufacturer. A typical experiment would use 3 mg (determined by UV) of NH6-TEV-ID#-EGFP/mRuby3 in 3 mL buffer (50 mM phosphate, pH 8.0, 100 mM NaCl), 1 mM DTT, and 10 μ L HaloTEV protease. The reaction would be monitored by SDS PAGE gel and was typically completed between 3-7 hr. The completed reaction solution was added to prewashed HaloLink resin for binding HaloTEV. After slowly rocking at RT for 30 min, the resin was filtered using an empty polypropylene column. The ID analogs were exchanged into buffer (50 mM phosphate, pH 8.0, 100 mM NaCl) using Amicon Ultra-15 filters to reduce DTT concentration to sub-micromolar levels and to remove the low molecular weight cleavage byproduct. Greater than 90% yields were typically achieved (~2.5 mg). Prior to all gel experiments, the proteins were dialyzed into 2X HBS buffer (50 mM HEPES, 300 mM NaCl, pH 7.4) using Amicon Ultra filters.

Expression of IFN α 5 analogs: The expression of IFN α 5 and its ID analogs followed a similar protocol as reported previously for type-I IFN α subtypes.¹ Briefly, the vector encoding IFN α 5 was transformed into BL21 Codon Plus DE3 RP cells (Agilent) and plated onto LB Agar containing 100 μ g/mL carbenicillin. The plates were grown overnight at 37 °C. Colonies were picked and

inoculated into 2 x 1 mL of LB with 1.0% glucose and 100 µg/mL carbenicillin. The cells were incubated at 37 °C and 250 RPM until turbid (2-3 hours). The cells were spun down, the supernatant removed, and the cells were resuspended into 2 x 1 mL of complete Studier ZYP-5052 media (taken from 1 L bottle, Teknova). The cells were transferred to the same 1 L bottle of Studier media and split into of 2 x 2.8 L flasks (~ 500 mL in each), then incubated at 37 °C and 250 RPM. OD₆₀₀ was monitored until reaching ~0.6, after which the flasks were shaken at 20 °C and 285 RPM for 20 hours. The culture was split into 2 x 500 mL centrifuge bottles and spun down for 30 min at 7000 g and 4 °C. The supernatant was removed and the pellets were stored at -80 °C until purification. For the ID analogs, the proteins were transformed into BL21 Codon Plus DE3 RP cells and grown on LB Agar plates overnight as above. However, proteins were not expressed in the soluble fraction during autoinduction. Therefore, single colonies were picked from the agar plates and inoculated 10 mL of LB (100 µg/mL carbenicillin). The cultures were grown overnight at 37 °C, 250 RPM. For each ID protein, 5 mL of overnight culture was used to seed 500 mL of LB (100 µg/mL carbenicillin), and the culture was shaken at 37 °C, 250 RPM. OD₆₀₀ was monitored until reaching a value of ~0.6, usually around 2-2.5 hr. IPTG was added to 1 mM and the cultures were continued to shake at 37 °C, 250 RPM for 5 hours, then spun down in 2 x 250 mL bottles for 30 min at 7000 g and 4 °C.

Purification of IFNα5 analogs: 1 x 500 mL pellet of IFNα was suspended in 40 mL lysis buffer (100 mM Tris-acetate pH 8.0, 100 mM sodium acetate, 1 mM EDTA). The sample was placed on ice and sonicated (25% amp, 1 s on, 1 s off, 2.5 min total on). The lysate was then centrifuged at 4 °C, 10,000 g for 30 min and the supernatant was syringe filtered (0.45 µm). Using a GE P-960 sample pump, the lysate was injected into a GE ATKA FPLC system equipped with a X16 column manually packed with 5 mL of Profinity eXact resin (Bio-Rad). The resin was washed with 15 CV of wash buffer (same as lysis buffer). 2 CV of elution buffer (100 mM Tris-acetate pH 8.0, 100 mM sodium acetate, 10 mM sodium azide) was passed over the resin, then the pump was stopped and the resin was allowed to incubate with the elution buffer for 30 min, after which an additional 10 CV was added. Fractions were checked by SDS-PAGE, combined, concentrated via Amicon Ultra filter, diluted into buffer containing 100 mM Tris-acetate and 20 mM NaCl, and loaded onto the FPLC equipped with a HiTrap Q HP 5 mL cartridge (equilibrated with 100 mM Tris-acetate and 20 mM NaCl). A gradient of 0-100% B (100 mM Tris acetate, 500 mM NaCl) over 20 CV was used. Fractions were checked by SDS-PAGE, combined, concentrated via Amicon Ultra filter, and then manually injected into the FPLC equipped with a HiPrep 26/60 Sephacryl S-200 HR size exclusion column equilibrated with 2X HBS. Fractions were checked by SDS-PAGE, combined, and concentrated using Amicon Ultra filters. Yield was ~ 3 mg per L culture.

For both ID analogs, 1 x 250 mL pellet was resuspended in 20 mL lysis buffer (for 50 mL buffer, 100 mM Tris-acetate pH 8.0, 100 mM sodium acetate, 0.5x bug buster, and 1 protease inhibitor tablet). The sample was placed on ice and sonicated (25% amp, 1 s on, 1 s off, 2.5 min total on). The lysate was then centrifuged at 4 °C, 10,000 g for 30 min and the supernatant was removed. The insoluble pellet was washed by resuspending in 20 mL 100 mM Tris-acetate pH 8.0, 100 mM sodium acetate (no bug buster), spun down, and buffer removed. 10 mL of the Tris-acetate buffer was added to the pellet and the cells were resuspended. The sample was sonicated on ice (25% amp, 1 s on, 1 s off, 1.0 min total on). Then 50 units of benzonase nuclease was added to the sample and rocked at RT for 1 hr. The sample was then spun down, the supernatant removed, resuspended in 20 mL Milli-Q water, spun down, water removed, and then resuspended in 10 mL

denaturing buffer (6 M guanidine HCl, 100 mM Tris-acetate, pH 8.0, 5 mM DTT). The sample was rocked at RT for 30 min, with intermittent vortexing, and then spun down. The denaturing solution was then added quickly to pre-chilled refolding buffer (490 mL, 100 mM Tris-HCl, pH 8.0, 50 mM NaCl, 2 mM reduced glutathione, 0.2 mM oxidized glutathione, 0.1 M arginine) and stirred at 4 °C overnight (~ 16 hr). The refolded protein was concentrated to ~ 25 mL using a Millipore Labscale TFF system equipped with a 10k MWCO Biomax Pellicon cassette. For IFN α -ID3, the protein was then dialyzed using 3.5k MWCO SnakeSkin dialysis tubing and 2 x 4L 20 mM Tris-acetate, pH 8.0, 100 mM urea (one exchange for 4 hour, the other overnight). The sample was spun down, syringe filtered (0.45 μ m), and incubated with 2 mL of pre-washed Profinity eXact resin by rocking at RT for 45 min. This was then loaded into an empty 20 mL polypropylene gravity column and washed with 10 CV of 100 mM Tris-acetate, pH 8.0, 100 mM sodium acetate. The sample was eluted using 10 CV of 2X HBS elution buffer (50 mM HEPES, 300 mM NaCl, pH 7.4, 10 mM sodium azide), with each CV incubated for 10 min at RT before the next addition of elution buffer. Pure fractions of IFN α -ID3 were combined, dialyzed into 2 x 4L of 2X HBS, then concentrated by Amicon Ultra filters. For IFN α -ID5, after TFF concentration the protein was dialyzed into 2 x 4L of 1X HBS (3 hr and overnight). The sample was syringe filtered and incubated with 0.8 mL Talon resin for 30 min, transferred to an empty 10 mL gravity column, then washed with 10 CV of 1X HBS containing 5 mM imidazole. The protein was eluted using 1X HBS supplemented with 200 mM imidazole. Pure fractions were combined and dialyzed into 2 x 4L 25 mM HEPES, pH 7.4, 50 mM sodium acetate. The protein was then incubated with 1.4 mL eXact resin, loaded onto an empty 20 mL gravity column, washed with 10 CV of 25 mM HEPES, 50 mM sodium acetate, then eluted over 7 CV of 2X HBS supplemented with 10 mM sodium azide (with each CV of elution buffer incubated for 10 min). The pure protein fractions were combined and dialyzed into 2 x 1L of 2X HBS, then concentrated by Amicon Ultra filters. Yield was 8-10 mg per L culture.

UV and Fluorescence Measurements

Protein stock concentrations in 2X HBS were determined by UV (EGFP: $\epsilon = 56,000 \text{ M}^{-1} \text{ cm}^{-1}$ at 488 nm; mRuby3: $\epsilon = 128,000 \text{ M}^{-1} \text{ cm}^{-1}$ at 558 nm; IFN α 5: $\epsilon = 18,700 \text{ M}^{-1} \text{ cm}^{-1}$ at 280 nm) using an Agilent 8453 UV-Vis spectrometer with a 1 cm cell and diluted to the designated 2X protein concentrations prior to mixing with peptide for gelation. For EGFP and mRuby analogs, fluorescence spectra were obtained using a Photon Technology International SpectroFluorometer and a 3 x 3 mm cell at sample concentrations of 30 nM. All ID-proteins exhibited similar absorbance and fluorescence properties as unmodified proteins.

In Vitro Gel Release Experiments

EGFP and mRuby3 release: AcVES3 was dissolved in cold Milli-Q water at 1.0 wt%. The peptide solution was vortexed for 30 s, chilled on ice for 10 min, and this process was repeated 2 more times to ensure complete dissolution of the peptide. 50 μ L of peptide solution was added to a pre-chilled glass vial, followed by the addition of 50 μ L pre-chilled protein (60 μ M in 2X HBS) – 3 vials were prepared for each protein. The vial was capped and the hydrogel was set for 1 hr at 37 °C, with a final gel composition of 0.5 wt% AcVES3 and 30 μ M protein in 1X HBS (25 mM HEPES, 150 mM NaCl, pH 7.4). After setting for 1 hr, 1 mL of 1X HBS was added to the top of the gel and the samples were incubated at 37 °C. At specified time points, the supernatant was removed and replaced with 1 mL fresh 1X HBS. The UV spectrum for each supernatant was taken to determine protein concentration, which was used to quantify the number of moles released per time point.

The cumulatively released protein amount was compared to the initial protein loading in the gel (# mol cumulatively released protein/ 3.0×10^{-9} mol loaded protein). Based on the UV spectra for each time point, the protein containing supernatant was diluted to 30 nM for fluorescence measurements and the spectra were normalized to that of the corresponding protein before hydrogel encapsulation. For co-encapsulation and subsequent release of EGFP and ID5-mRuby3, the final concentration of each protein loaded into the gel was 15 μ M (total protein content was 30 μ M, the same as for individual protein release experiments). A demonstration of the mixing and gelation process is shown in Video S1.

IFN α 5 release: AcVES3 was prepared at 2.0 wt% in cold Milli-Q, as described above. The peptide solution was vortexed for 30 s, chilled on ice for 10 min, and this process was repeated 2 more times to ensure complete dissolution of the peptide. 50 μ L of peptide solution was added to a pre-chilled glass vial, followed by the addition of 50 μ L pre-chilled protein (150 μ M in 2X HBS) – 3 vials were prepared for each protein. The vial was capped and the hydrogel was set for 1 hr at 37 °C, with a final gel composition of 1.0 wt% AcVES3 and 75 μ M protein in 1X HBS (25 mM HEPES, 150 mM NaCl, pH 7.4). After setting for 1 hr, 1 mL of 1X HBS was added to the top of the gel and the samples were incubated at 37 °C. At specified time points, the supernatant was removed and replaced with 1 mL fresh 1X HBS.

HL116 Cell Activity Assays

The HL116 luciferase assays followed a similar protocol as reported previously for type-I IFN α subtypes.¹ Briefly, HL116 cells were cultured in DMEM-glutamax media containing 10% FBS and incubated at 37 °C with 5% CO₂ and humidity control. The cells were trypsonized and then diluted to 4×10^5 cells/mL. 100 μ L of diluted cells was pipetted into wells of a white 96 well plate (4×10^4 cells per well), then grown overnight. The next day, serial dilutions of IFN α 5 analogs were prepared in pre-heated DMEM-glutamax (1 – 1000 pM). The culture media was removed from the cells and replaced with 100 μ L of the appropriate protein concentration (in triplicate), then incubated for 5 hrs. The plates were then removed from the incubator and allowed to equilibrate to room temperature (~15 min). 100 μ L of Steady-Glo Luciferase assay reagent (Promega) was added to the cells, gently rocked, and incubated for 5 min at room temperature. The luminescence was read by a Biotek Neo2 plate reader.

For the HL116 activity assays using gel-released protein, 0.5 wt% peptide gels containing either 5 μ M IFN α 5-ID5 or no protein in 1X HBS were prepared in transwell inserts. The inserts were placed into a clear, non-treated 24 well plate and set for 1 hr at 37 °C (3 gels were prepared for each condition). After setting the gel, 0.5 mL of DMEM-glutamax was added to the top of the gels and 0.5 mL was added to the bottom of the wells. The gels were incubated with media for 1 day (37 °C with 5% CO₂ and humidity control). In separate white plates, cells were plated as described above and grown overnight. The next day, the media was removed from the cells and 2 x 100 μ L aliquots from each gel condition was added (N = 6) to the white plates with cells. Untreated cells (negative control) or media containing 500 pM IFN α 5 (positive control) were also added to the white plates with cells (N = 3). The plates were incubated for 5 hrs and then equilibrated to room temperature. 100 μ L of Steady-Glo Luciferase assay reagent was added to the cells, gently rocked, incubated for 5 min at room temperature, and then the luminescence was read.

Oscillatory Rheology

Rheological assessment was conducted on a Texas Instruments AR-G2 rheometer using a 25 mm stainless steel parallel geometry. A representative set of ID-EGFP proteins was used to determine whether the interaction domain affected the material properties of AcVES3 hydrogels. 0.5 wt% gels were prepared as described in the previous sections for gel release, with 150 μL of chilled AcVES3 solution mixed with 150 μL pre-chilled 2X HBS solution (containing 60 μM protein, 200 μM protein, 340 μM protein, or just buffer). This solution (0.5 wt% AcVES3 with 0/30/100/170 μM protein) was immediately applied to the center of the plate and the upper geometry was lowered to a gap height of 0.5 mm. The temperature was increased from 5 $^{\circ}\text{C}$ to 37 $^{\circ}\text{C}$ over 100 s at a constant angular frequency of 6 rad s^{-1} and 0.2% strain. The storage and loss moduli were monitored for 60 min at a constant angular frequency of 6 rad s^{-1} and 0.2% strain at 37 $^{\circ}\text{C}$. After the time sweep, dynamic frequency sweeps (0.1-100 rad s^{-1} at constant 0.2% strain) and strain sweeps (0.1-1000% strain at constant 6 rad s^{-1}) were performed to ensure that time sweep data were collected in the linear viscoelastic regime. Shear-thinning experiments were carried out in duplicate. Fresh samples were applied to the plate, the geometry was lowered, and the temperature was increased from 5 $^{\circ}\text{C}$ to 37 $^{\circ}\text{C}$. The moduli were monitored for 60 min (6 rad s^{-1} , 0.2% strain, 37 $^{\circ}\text{C}$), followed by the application of 1000% strain for 30 s to shear the gel, after which the strain was reduced to 0.2% and the gel was allowed to recover for 60 min (6 rad s^{-1} , 0.2% strain).

Circular Dichroism

CD spectra of AcVES3 peptides were collected on an Aviv Model 420 Spectrometer. 0.5 wt% peptide gels were prepared as described previously by mixing together 100 μL 1 wt% peptide in water with 100 μL 2x HBS, and adding 175 μL to a 0.1 mm cuvette. The sample was then placed into the instrument holder pre-heated to 37 $^{\circ}\text{C}$ and allowed to gel for 1 hr. Wavelength scans were then carried out at 37 $^{\circ}\text{C}$ between 260 and 200 nm at 1 nm intervals, with an averaging time of 3 sec at each wavelength. A background spectrum of 1x HBS was subtracted from the sample spectra and the mean residue ellipticity $[\theta]$ was calculated from the equation $[\theta] = (\theta_{\text{obs}}/10lcr)$, where θ_{obs} is the measure ellipticity in millidegrees, l is the length of the cell in centimeters (0.01 cm), c is the molar concentration (0.0022 M), and r is the number of peptide bonds (21). CD was also conducted on the 0.5 wt% solution of the soluble peptide in water.

CD spectra of IFN α 5 proteins were collected on a Jasco J-1500 Spectrometer. Proteins were diluted to 5 μM in 0.5x HBS and wavelength scans were carried out at 25 $^{\circ}\text{C}$ between 260 and 200 nm at 1 nm intervals, with an averaging time of 2 sec at each wavelength and 5 experiments each. A background spectrum of 0.5x HBS was subtracted from the sample spectra and the mean residue ellipticity was calculated as described above ($l = 0.1$ cm; $c = 0.000005$ M; $r = 168$ for IFN α 5, 185 for IFN α 5-ID3, and 189 for IFN α 5-ID5).

Transmission Electron Microscopy

TEM images were collected on an FEI T12 microscope at 80 kV. 50 μL of 0.5 wt% AcVES3 gels were prepared as described previously and set overnight at 37 $^{\circ}\text{C}$. Gels were made for empty AcVES3, AcVES3 + 50 μM ID5-EGFP, and D-AcVES3. The next day, 2 μL of gel was removed and diluted into 78 μL water (40x dilution), with gentle aspiration and stirring with the pipet tip. 4 μL of this solution was then applied to a glow discharged, carbon-filmed, 400 mesh copper grid (Electron Microscopy Sciences). After 1 min the excess solution was blotted, then the sample was

washed twice with 4 μ L water, and stained four times with 4 μ L 1.0% uranyl acetate solution. After the fourth application, the stain was applied for 1 min before blotting. Multiple locations on the grid were imaged, which were analyzed using the software Image J (NIH) to determine fiber width.

In Vivo Gel Release Experiments

Hydrogels were prepared in an identical manner as described for the in vitro experiments (0.5 wt% AcVES3, 30 μ M mRuby3/ID5-mRuby3 in 1X HBS), except that after mixing the peptide and protein components the solution was immediately drawn into a 1 mL syringe and the gel was set at 37 °C for 1 hr. Each syringe contained multiple 100 μ L doses. Animal studies were performed according to the Frederick National Laboratory for Cancer Research Animal Care and Use Committee guidelines. Fluorescence imaging was performed on non-tumor bearing 6-8-week-old female athymic nude mice (Charles River Laboratories, Frederick, MD). 100 μ L of protein loaded hydrogel was administered by subcutaneous injection into either the left or right flank for each mouse and imaged at various time-points post injection. Mice body temperature were kept constant during the procedure with a heated pad located under the anesthesia induction chamber, imaging table, and post procedure recovery cage all maintained at 37 °C. Anesthesia was initially set at 3% isoflurane with filtered (0.2 μ m) air at 1 liter/minute flow rate for 3-4 minutes and then modified for imaging to 2% with O₂ as a carrier with a flow rate 1 liter/minute. Mice were fluorescence imaged using the IVIS SPECTRUM (PerkinElmer Inc., Waltham, MA) at the specified time-points in the prone position. Static 2D images were acquired with the following parameters: excitation filter 570 \pm 15 nm, emission filter 620 \pm 10 nm, f/stop 2, medium binning (8X8) and auto exposure (typically 1-60 seconds). Acquisition and analysis were performed with vendor specific software Living Image (version 4.3.1) (PerkinElmer Inc, Waltham, MA). Circular regions of interest (ROI) were drawn on the injection site to evaluate the presence of fluorescent protein within the hydrogel over time by monitoring the change in total radiance efficiency (photons/second/cm²/steradian/mW). The three groups of mice contained the following - Group 1: 3 mice, all injections used L-AcVES3 hydrogels, left flank gel contained mRuby3, right flank gel contained ID5-mRuby3; Group 2: 3 mice, all injections used D-AcVES3 hydrogels, left flank gel contained mRuby3, right flank gel contained ID5-mRuby3; Group 3: 5 mice, all injections used ID5-mRuby3, left flank used L-AcVES3 hydrogel, right flank used D-AcVES3 hydrogel. At the end of the study, animals were euthanized by CO₂ asphyxiation.

Histological Analysis of Injection Site Tissue

Immediately following euthanasia, group 3 mice were processed for histology. Approximately 2 cm² sections of skin and the underlying subcutis and peritoneal wall were harvested from the injection sites on the left and right dorsal flanks. The tissues were fixed in 10% neutral buffered formalin for 24 hours, following which they were trimmed and submitted to Histoserv in 70% ethanol for routine processing. A minimum of five sections per injection site were embedded in paraffin, sectioned at 5 μ m, and stained with hematoxylin and eosin. All sections were evaluated by a board-certified veterinary pathologist using an Olympus BX40 microscope. Figure 8C/D in main text is a representative example showing the correlation between a detected fluorescent signal for ID5-EGFP-loaded gels and the presence of gel remaining in the tissue for mouse 2 of group 3 (Figure 8B, and 2nd from left in Supporting Figure S16C).

Modelling the AcVES3 fiber/ID interaction

After building initial models of the AcVES3 fiber and the interaction domains (IDs), all molecular dynamics (MD) simulations were performed using a GPU accelerated version of the program Amber16² and the conditions summarized in supporting Table S1.

An initial model of the AcVES3 fiber was built based on the experimental structure for assembled MAX1 (PDB: 2N1E).³ Possible arrangements Syn/Syn, Syn/Anti, Anti/Anti, Anti/Syn were generated by repositioning the AcVES3 peptides in the appropriate orientations. Geometry optimization was performed by simulated annealing of the four models. The energy differences among the four forms suggests the Syn/Anti arrangement is favored (1.3 kcal/mol over the second most stable geometry Anti/Syn), which is in agreement with the observed orientation in the MAX1 structure. An idealized extended model of the fiber was generated by propagating the Syn/Anti dimer using translation and pitch angles from MAX1, which were then energy optimized for the AcVES3 sequence using the program X-plor-NIH (Figure S13).⁴ All AcVES3 fiber and fiber/ID models were relaxed in a solvent box containing Na⁺ as the charge neutralizing ion and NaCl (150 mM). Modeling conditions are summarized in Table S1. Relaxation of the initial models was performed by applying a soft restraint to the C_α atoms (0.2 kcal/mol-Å²) in Amber16, which keeps the fiber elongated during the simulations.

Initial ID models (ID1 to ID6) were built using VMD⁵ Molefacture plugin. ID conformations were generated using molecular dynamics in a simulated continuum solvent model (1 microsecond total simulation time per ID.) The conformations obtained during the MD simulations were clustered (RMSD) from samples extracted every 5 ns considering the Ca atoms only. The geometries with the lowest energy from each cluster were relaxed in an explicit solvent box. The relaxed conformations with the lowest energies were docked against the fiber model using the program ZDOCK.⁶ The IDs contain a linker sequence that would be attached to a protein of interest (sequence GGSGSGGSGS), and is referred to here as the ID-linker. Docking was performed without including the ID-linker, which allowed for a more thorough exploration of the ID – fiber interaction poses. Poses that may occlude the ID-linker were subsequently excluded. ZRANK⁶ was used as a first criterion to select the more favorable poses, and it was determined that all IDs bound to the fiber in an extended conformation. Selected poses were further refined using short (up to 25ns) MD trajectories followed by energy minimization. The binding energies of the ID-fiber interactions was then explored using the Linear Interaction Energy (LIE) method,⁷ with each LIE reported in Figure 6A of the main text. A more detailed explanation of the LIE parameters can be found below in the next section. From the LIE data, it was observed that ID1/ID2 are poor binders and ID3-6 are strong binders. When the IDs were forced to engage the fibers in compact states, the LIEs were also determined to be weak. For example, six compact forms of ID6 were used, with the average energy of all compact forms being ~36 kcal/mol less favorable than the extended conformations of ID6. To further explore the preferred binding of an extended form of ID6, the relative energetics of compact/extended conformations in solution (unbound to the fiber) was determined using $\Delta G_{\text{compact}} = -kT \log (f_c / f_e)$, with f_c the fraction of compact forms and f_e the fraction of elongated forms observed. Two independent 25ns MD trajectories starting from each conformation were used to obtain f_c and f_e , resulting in $\Delta G_{\text{compact}} = -2.4$ kcal/mol, which is not sufficient to compensate for the compact form's substantially lower binding energy. The favoring of the extended form can be rationalized because it reduces Arg-Arg side chain repulsion and maximizes the potential for making non-competing Arg-Glu

interactions (i.e. Arg side-chain interacting with Glu side chains not interacting with other Arg side chains.). All subsequent simulations were performed using the more favorable ID elongated poses as the initial conformations.

After the initial docking, additional experiments were conducted in which the repulsion forces between a negatively charged protein and the negatively charged fiber were mimicked. Here, a simple model was used to simulate a smooth "extraction" of the ID from its attached conformation. Proteins have a characteristic translational diffusibility $\sim 1 \text{ (cm}^2\text{s}^{-1}) \times 10^6$,⁸ which is much slower than the processes simulated here. Thus the "pull" of a protein against the ID was simulated by stretching the ID-linker while retaining the ID bound portion in place, then relaxing the entire system using a soft 2 kcal/mol restraint applied to the C termini of the ID-linker (where the ID would be attached to the protein). The relaxation of the ID-linker geometry produces a very gentle pull that is sufficient to dislodge ID1 from the fiber, while minimally affecting the binding of ID6, further confirming the differences between the short and long IDs. Video S2 shows the side-by-side "pull" experiments for ID1 and ID6. The analysis of the diffusibility of the ID on the fiber during the "pull" experiments may further differentiate the ID-family members. The diffusion coefficient (D) is related to the mean displacement ($\langle r \rangle$) over a period of time (t) by $\langle r \rangle = \sqrt{2nDt}$ for a system of dimensionality (n). The measured displacement was computed from the average center point of the Arg guanidinium groups in the ID. This approach for measuring the displacement removes the noise due to ID internal displacements. The change in the center of mass for the IDs can also assess mobility. Here, the center position between the terminal guanidino functionalities for each ID was monitored over time as it moves along the fiber from its initial docked position.

Binding Energies using the LIE method

Several methods of estimating interaction energies were considered,⁹⁻¹¹ but ultimately chose the LIE approach for a simple, qualitative description of the interaction. LIE methods are good at predicting binding energy when properly calibrated.^{7, 12} LIE methods use a semi-empirical expression to describe the binding interaction:

$$\Delta G_{bind} = \alpha \Delta E_{vdW} + \beta \Delta G_{elec} + \gamma \Delta A + \delta$$

α , β , γ and δ are adjustable constants. ΔE_{vdW} is the Van der Waals interaction energy between the fiber and an ID peptide. Van der Waals solvent-solvent contributions are ignored, leading to a great reduction in the energy noise level. ΔG_{elec} is the difference in electrostatic energy between the bound and unbound forms. The electrostatics term was calculated using a GB correction as described by Hawkins and coworkers.¹³ ΔA is the molecular surface change when the complex is formed and δ is a constant whose value can be calibrated. All energies are calculated along the MD path. The differences are simply calculated by separating the fiber and the peptide and calculating the energies of the complex and the separated fiber and peptide. This approach is known as a "single-path" approach and an estimation of the validity of this approximation is presented below.

The values of the adjustable parameters α , β and γ were obtained from the literature.^{12, 14-18} Published parameters were assessed against experimental binding energies for polypeptides

containing Arg, Lys, and Orn (ornithine) vs. Glu and Asp.¹⁹ This analysis was carried out using molecular dynamic simulations of the peptides in an explicit solvent using a treatment similar to that used for AcVES3 - ID systems. The best results were obtained with $\alpha = 0.2$; $\beta = 0.26$; $\gamma = -2$; $\delta = -1.3$. These parameters produce the following interaction energies (in kcal/mol and per monomer; experimental values in brackets): Poly-Lys / Poly-Asp 7.2 (6.8); Poly-Lys / Poly-Glu 7.5 (7.3); Poly-Orn / Poly-Asp 6.0 (6.2); Poly-Orn / poly-Glu 6.2 (6.8); Poly-Arg / poly-Asp 11.2 (> 9.6); Poly-Arg / Poly-Glu 12.0 (> 9.6).

The GB/LIE binding energies calculated for each ID / AcVES3 complex are summarized in main text Figure 2A. Calculated statistical errors were obtained by dividing each MD path into sets of 5 ns each from where the uncertainty estimate for ΔG was then $\sigma(\Delta G) = \text{SQRT}(\text{var}(\Delta G)/(N-1))$ with N the number of sets. All uncertainties were between 1.3 and 2.5 kcal/mol (ID6, ID3) suggesting that the length of the simulations provided sufficient sampling. Systematic cross-validation tests were used to assess the reliability of these results. This test was performed by dividing the data into eight randomly equal subgroups, with one subgroup being omitted at the time. This resulted in a variability range for uncertainties in the range 0.8 to 1.5 kcal/mol (ID6, ID3). These two errors were combined to produce a maximum bound for the total error estimate. This approach will overestimate the actual error but provides assurance that the trends observed may be valid.

Analyzing the MD Simulation Data to provide molecular level insight into ID-Fiber binding

Visual examination of the MD trajectories suggests a great variability in the interaction between the Arg side chains and Glu side chains from very low mobility Args with their side chains anchored to the fiber for extended periods of simulated time, to highly mobile Arg side chains. Based on this observation, the Arg geometries were categorized into three groups: weak (type I, 0 to -5 kcal/mol), intermediate (type II, -5.0 to -10 kcal/mol), and strong (type III, -10 to -15 kcal/mol) binding. To assign a type, the trajectories were divided into sections of 5 ns and the LIE for each Arg residues was computed. The 5ns trajectory section is necessary to compute a minimal LIE statistical model. For determining the positional preferences of a second type III binding interaction that occurs simultaneously with another, a sliding window (5ns) was run and each type of Arg interaction was computed within the frame for each Arg position. The pairs of type III interactions were counted, along with their relative positions, and the data was normalized across all IDs.

EGFP

MVSKGEELFTGVVPILVELDGDVNGHKFSVSGEGEGDATYGKLTCLKFICTTG
KLPVPWPTLVTTLTLYGVQCFSRYPDHMKQHDFFKSAMPEGYVQERTIFFKD
DGNKYKTRAEVKFEGDTLVNRIELKGIDFKEDGNILGHKLEYNNSHNVIYMA
DKQKNGIKVNFKIRHNIEDGSVQLADHYQQNTPIGDGPVLLPDNHYLSTQS
ALSKDPNEKRDHMLVLEFVTAAGITLGMDELYK

mRuby3

MVSKGEELIKENMRMKVVMESVNGHQFKCTGEGEGRPYEGVQTMRIKVI
EGGPLPFAFDILATSFMYGSRTFIKYPADIPDFFKQSFPEGFTWERVTRYED
GGVVTVTQDTSLEDGELVYNVKVRGVNFPSPNGPVMQKKTGKWEPTNEMM
YPADGGLRGYTDIALKVDGGGHLHCNFTTYRSKKTGNIKMPPGVHAVDH
RLERIEESDNETYVVQREVAVVKYSNLGGGMDELYK

ID1 fusion

GRHRGGSGSGSGSGS – (EGFP)

ID3 fusion

GRHRHRHRGGSGSGSGSGS – (EGFP)

ID5 fusion

GRHRHRHRHRHRGGSGSGSGSGS – (EGFP/mRuby3)

ID6 fusion

GRHRHRHRHRHRHRGGSGSGSGSGS – (EGFP)

NH6 fusion

MRS GSHHHHHRS DITSLYKKVGIEGR – (EGFP)

ID2 fusion

GRHRHRGGSGSGSGSGS – (EGFP)

ID4 fusion

GRHRHRHRHRGGSGSGSGSGS – (EGFP)

H6 fusion

HHHHHHGGSGSGSGSGS – (EGFP)

H12 fusion

HHHHHHHHHHHHGGSGSGSGSGS – (EGFP)

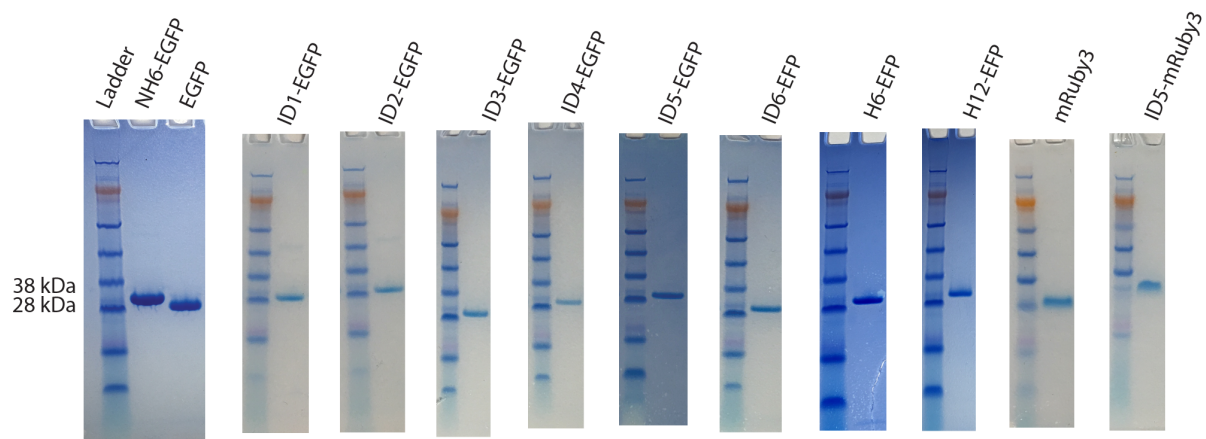
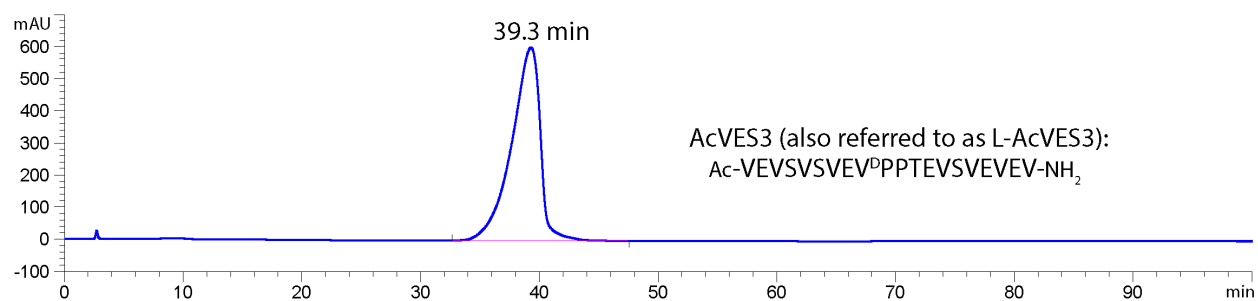


Figure S1. Sequences and SDS-PAGE gels for fluorescent proteins used in this study. pDest527-based vectors result in proteins expressed with an N-terminal peptide sequence containing a His-6 metal affinity chromatography handle. The FXa cleavage site (IEGR) was incorporated into NH6 for generating native EGFP and mRuby3. For ID-containing proteins, the TEV protease cleavage site (ENLYFQG) was incorporated into the vectors between the pDest527 His-6 containing sequence and the designed sequence for interacting with the hydrogel network. Cleavage by TEV protease result in a residual N-terminal Gly residue.



	MS (m/z)		
	calc.	obs. AcVES3	obs. D-AcVES3
(m-2H) ²⁻	1075.6	1075.5	1075.5
(m-3H) ³⁻	716.7	716.7	716.8
(m-4H) ⁴⁻	537.3	537.4	537.1

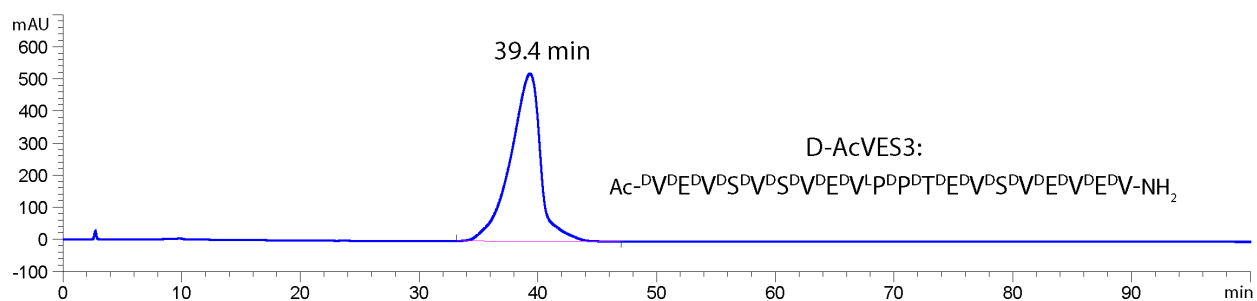


Figure S3. Analytical HPLC for AcVES3 and D-AcVES3, with tabulated mass spec data.

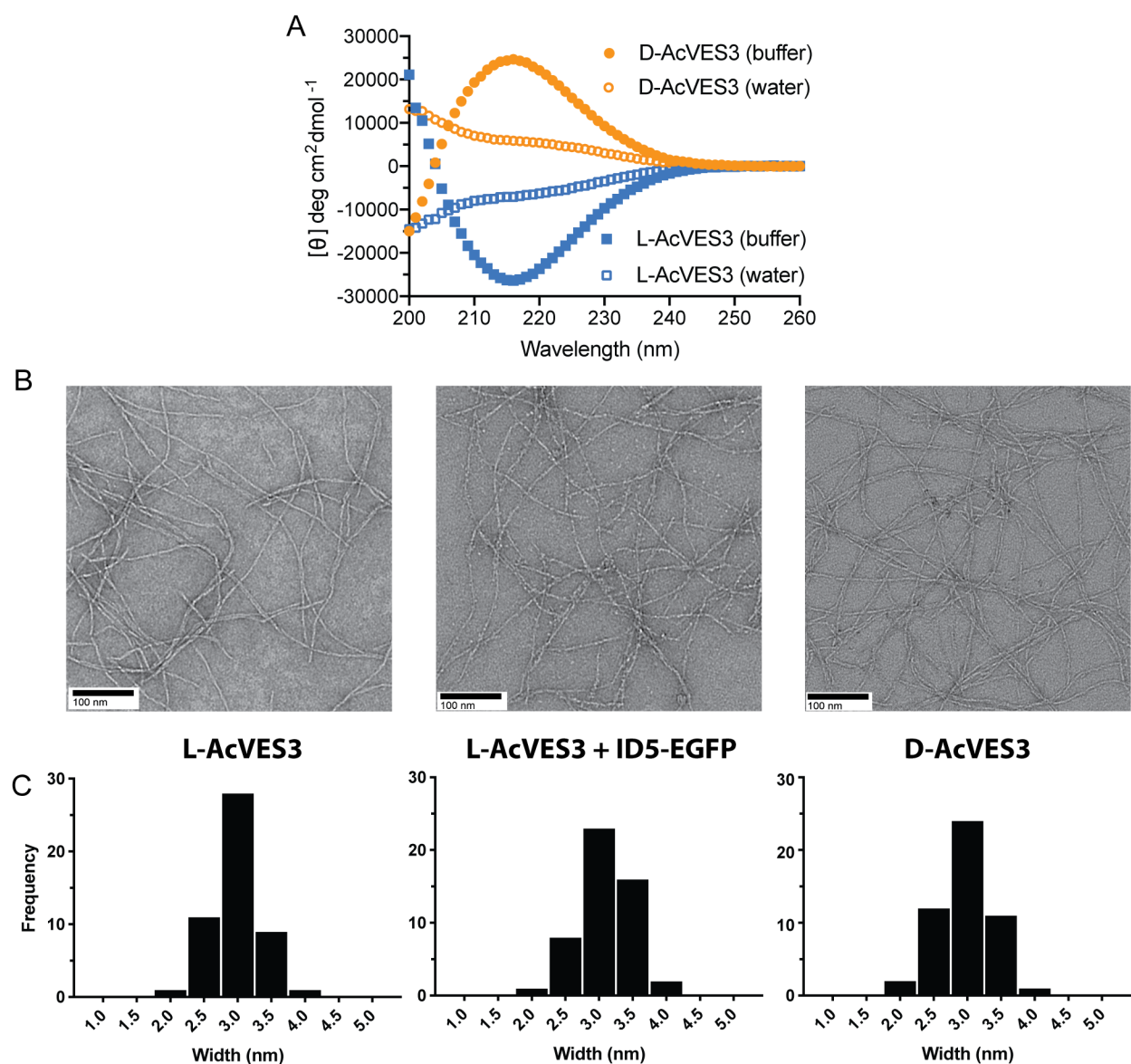


Figure S4. Structural analysis of AcVES3. A) CD of 0.5 wt% AcVES3 in either water (soluble, unfolded) or in buffer (folded, hydrogel state). B) Representative TEM images for L-AcVES3, L-AcVES3 + ID5-EGFP, and D-AcVES3, with 100 nm scale bar. C) Width dimensions of the AcVES3 fibers shown in (B) (N = 50), binned at ± 0.25 nm of centered value. Most fibers are ~ 3 nm wide, which is consistent with the length of a folded hairpin.

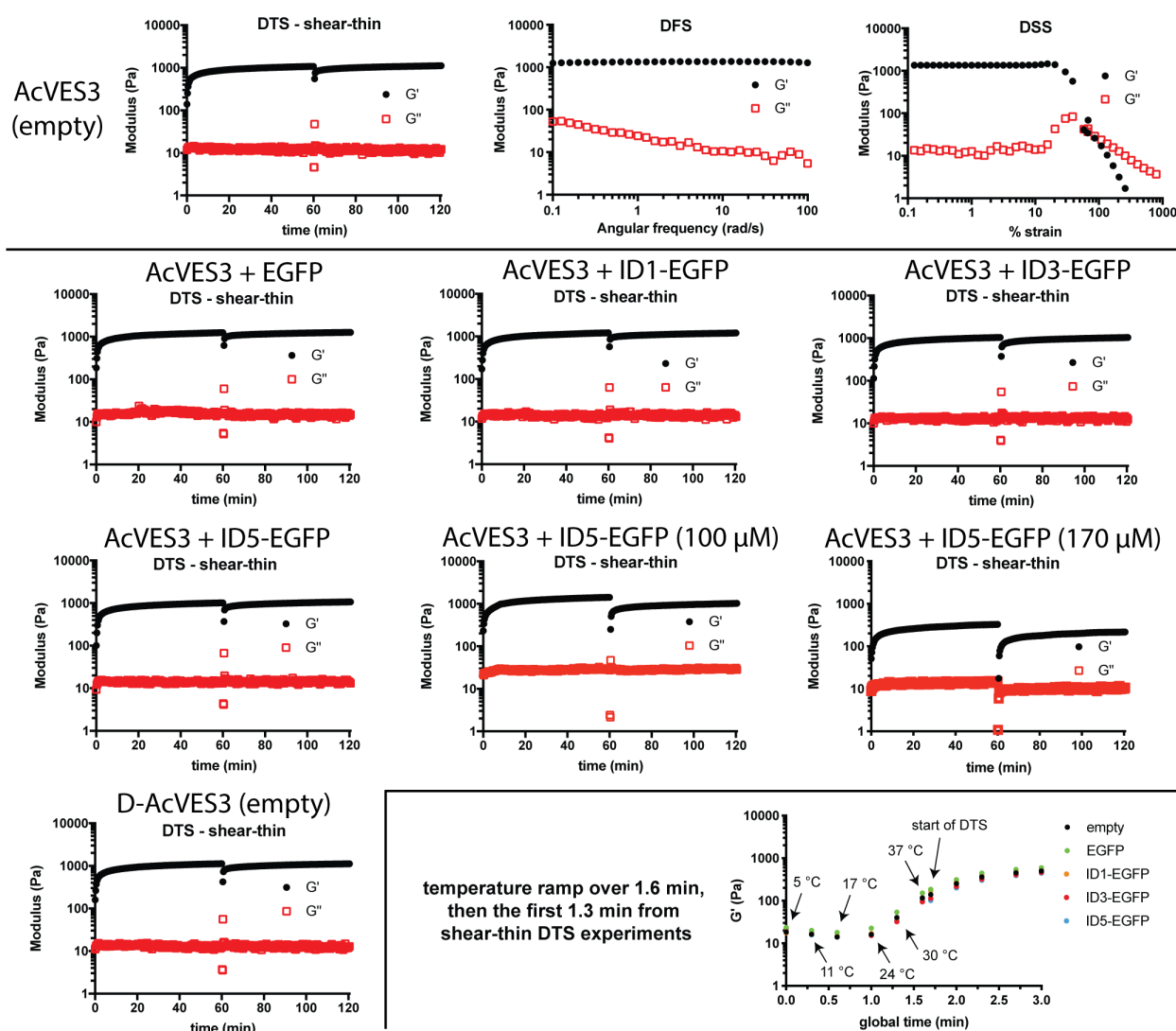


Figure S5. Rheology of empty and protein loaded hydrogels. Storage modulus (G') in filled-in circles, loss modulus (G'') in red open squares. For all experiments, hydrogel consisted of 0.5 wt% peptide. Protein concentration was 30 μ M (~ 1 mg/mL), except in the instance where 100 μ M (~3 mg/mL) or 170 μ M (~ 5 mg/mL) ID5-EGFP was used to demonstrate that higher ID-protein concentrations can be accommodated for shear-thin delivery. Shear-thinning dynamic time sweep (DTS) were performed at a constant angular frequency of 6 rad s⁻¹ and 0.2% strain for 60 min, followed by 1000% strain for 30 sec, and a 60 min recovery period. Dynamic frequency sweep (DFS) were performed at a constant 0.2% strain. Dynamic strain sweep (DSS) were performed at a constant angular frequency of 6 rad s⁻¹. Before each DTS experiment, there was a temperature ramp from 5 – 37 °C. In addition to the overall storage modulus being similar for empty and ID-containing gels after 1 hour, the early kinetics of gelation were also very similar.

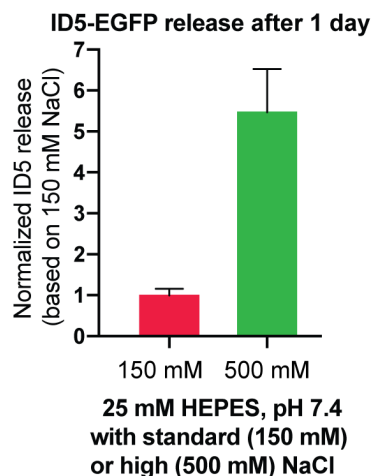


Figure S6. Effect of high salt content on the release of ID5-EGFP. After 1 day, the higher salt condition has more than 5x the release as the standard salt condition, suggesting that charge screening can alter the interaction between the ID and peptide gel and lead to faster release.

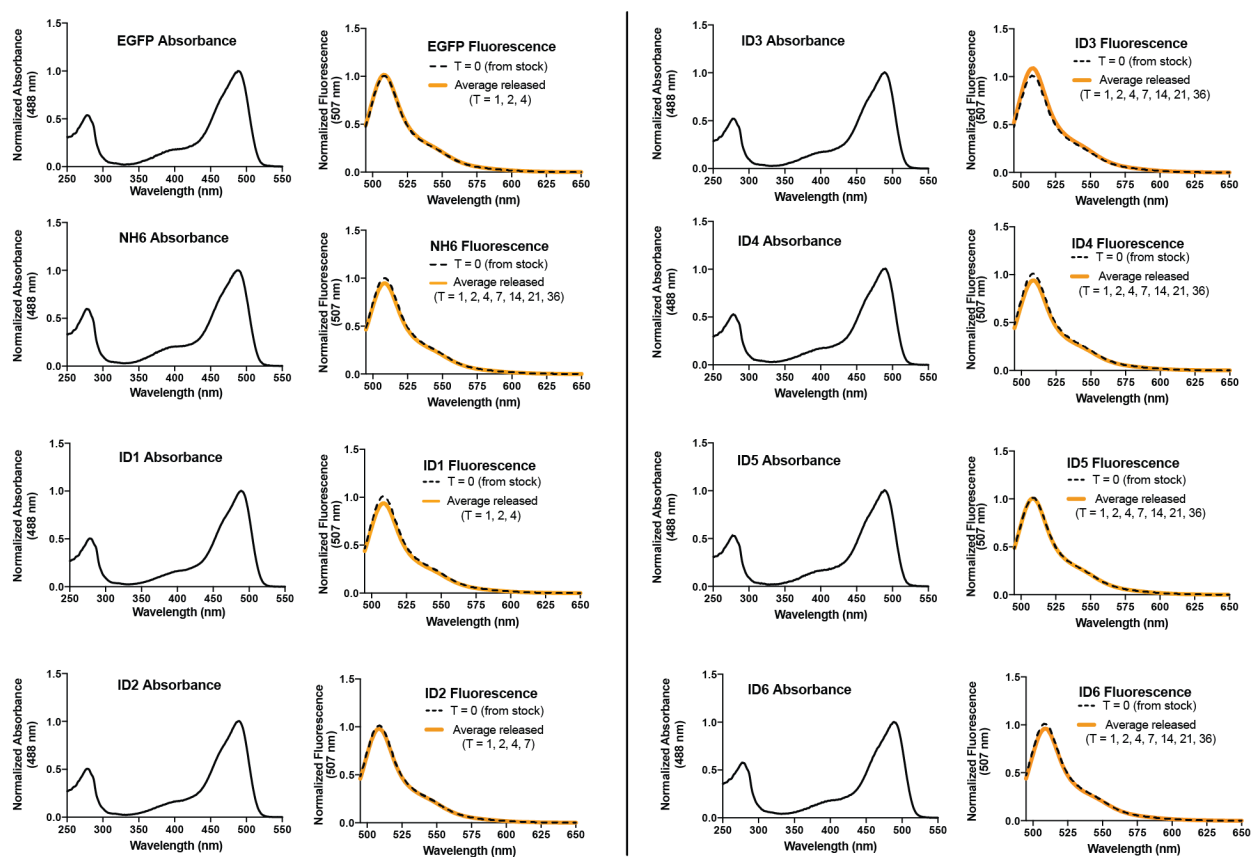


Figure S7. Normalized absorbance and fluorescence spectra for EGFP analogs. Absorbance normalized at 488 nm; fluorescence normalized at 507 nm.

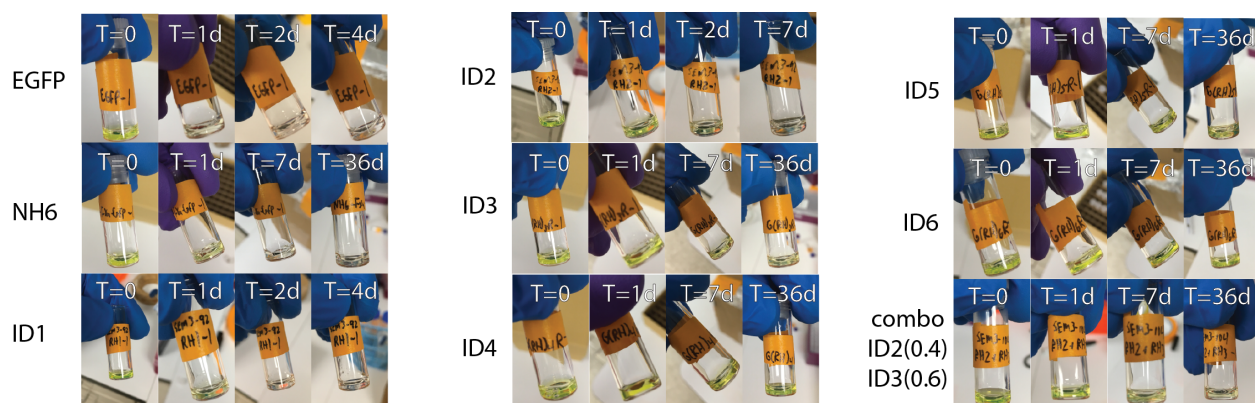


Figure S8. Images of EGFP loaded hydrogels at selected time points. Proteins with longer IDs displayed colored gels for entire length of study, indicating the presence of active EGFP.

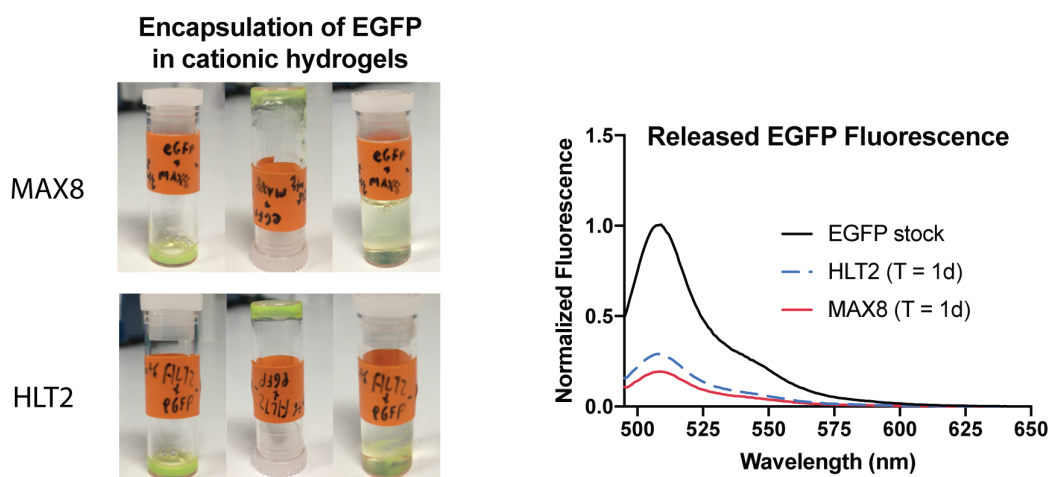


Figure S9. Encapsulating EGFP into positively charged hydrogels formed from cationic self-assembling peptides. MAX8: VKVKVKVKVDPLPTKVEVKVKV; HLT2: VLTQVKTKVDPLPTKVEVKVLV. The strong electrostatic interactions between negatively charged EGFP and two different cationic hydrogels resulted in cloudy, precipitated materials where the gel fell apart easily upon the addition of buffer. Protein released from these materials had a significant loss in fluorescence activity, indicating that denaturation had occurred.

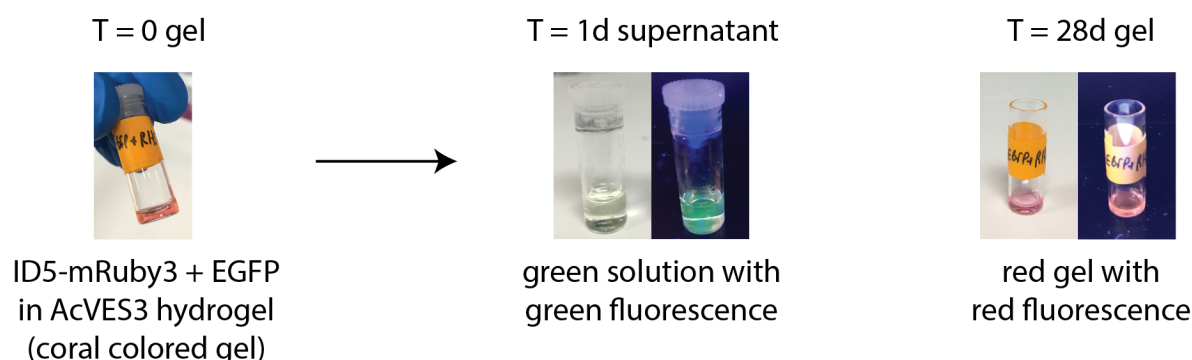


Figure S10. Image of co-encapsulated EGFP and ID5-mRuby3 in AcVES3 hydrogel. After 1 day, the supernatant exhibits a strong green fluorescence using a handheld UV lamp, while the gel retains a strong red fluorescence after 28 days. These qualitative visual results support the quantified data in main text Figure 4B.

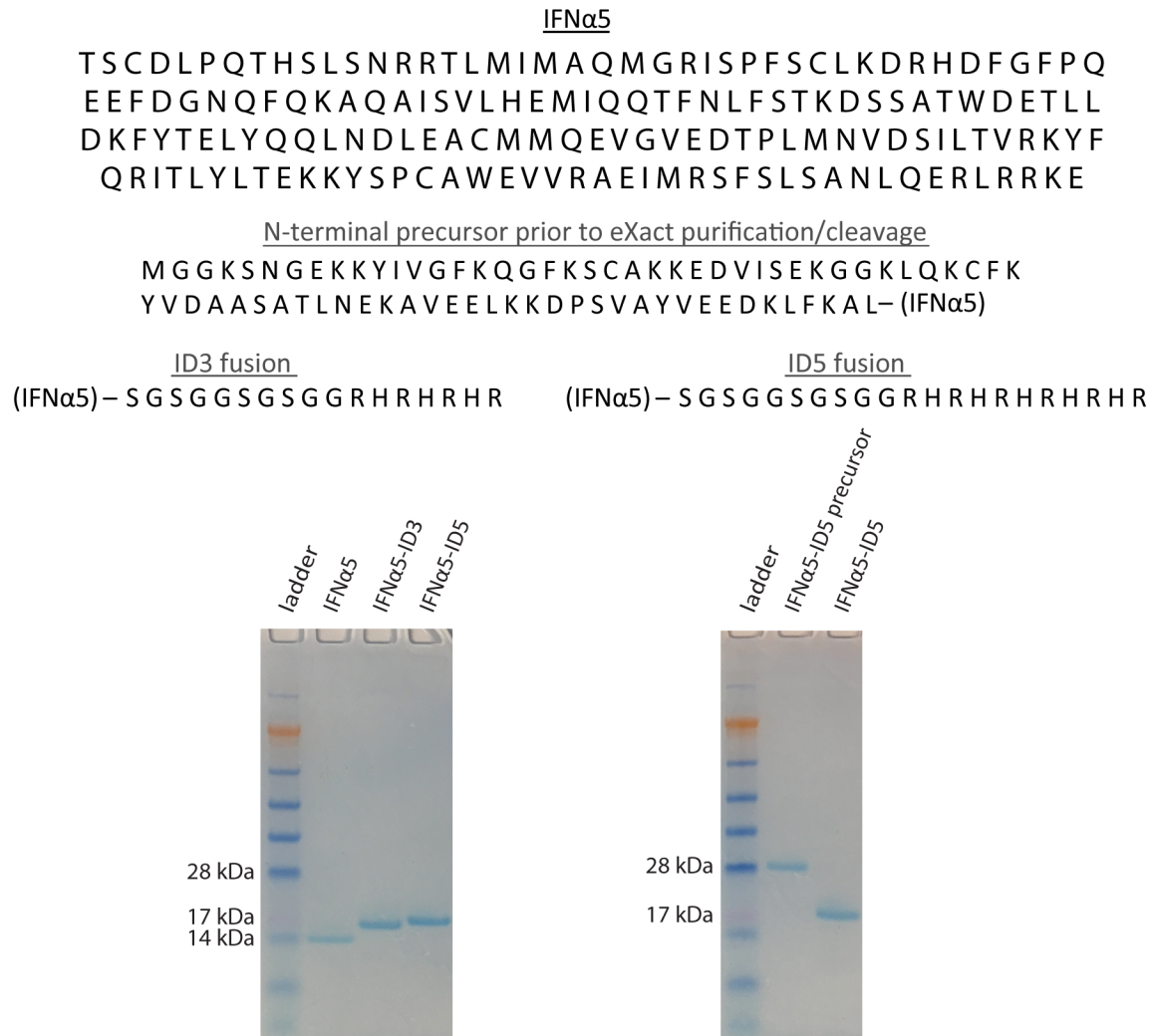


Figure S11. Sequences and SDS-PAGE gels for IFN α 5 and its ID analogs. Here, the ID is appended to the C-terminus of the protein. IDs were cloned into the pPAL7 vector already containing IFN α 5. The precursor proteins are expressed with an N-terminal domain that binds to the analog of subtilisin protease bound to the Profinity eXact resin and can be washed to remove protein impurities. The proteins are then eluted/cleaved in buffer containing 10 mM NaN₃. Longer IDs, which may be favorable for slow release protein formulations, contain enough histidine residues to purify by metal affinity without the need for an additional poly-histidine domain. We demonstrate this proof-of-concept by purifying the precursor of IFN α 5-ID5 with Talon resin prior to subjection to the eXact resin.

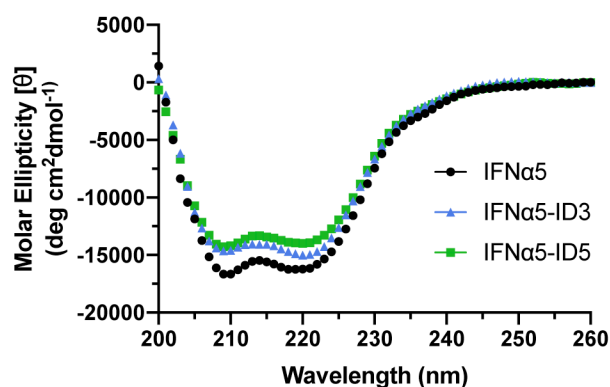


Figure S12. CD spectra of IFN α 5 analogs. All proteins exhibit robust helical conformations. The unstructured nature of the IDs (ID3: 17 residues; ID5: 21 residues), however, causes the helical signature of the mean residue ellipticity to be slightly less intense due to the increased contribution of random coil to the overall spectra.

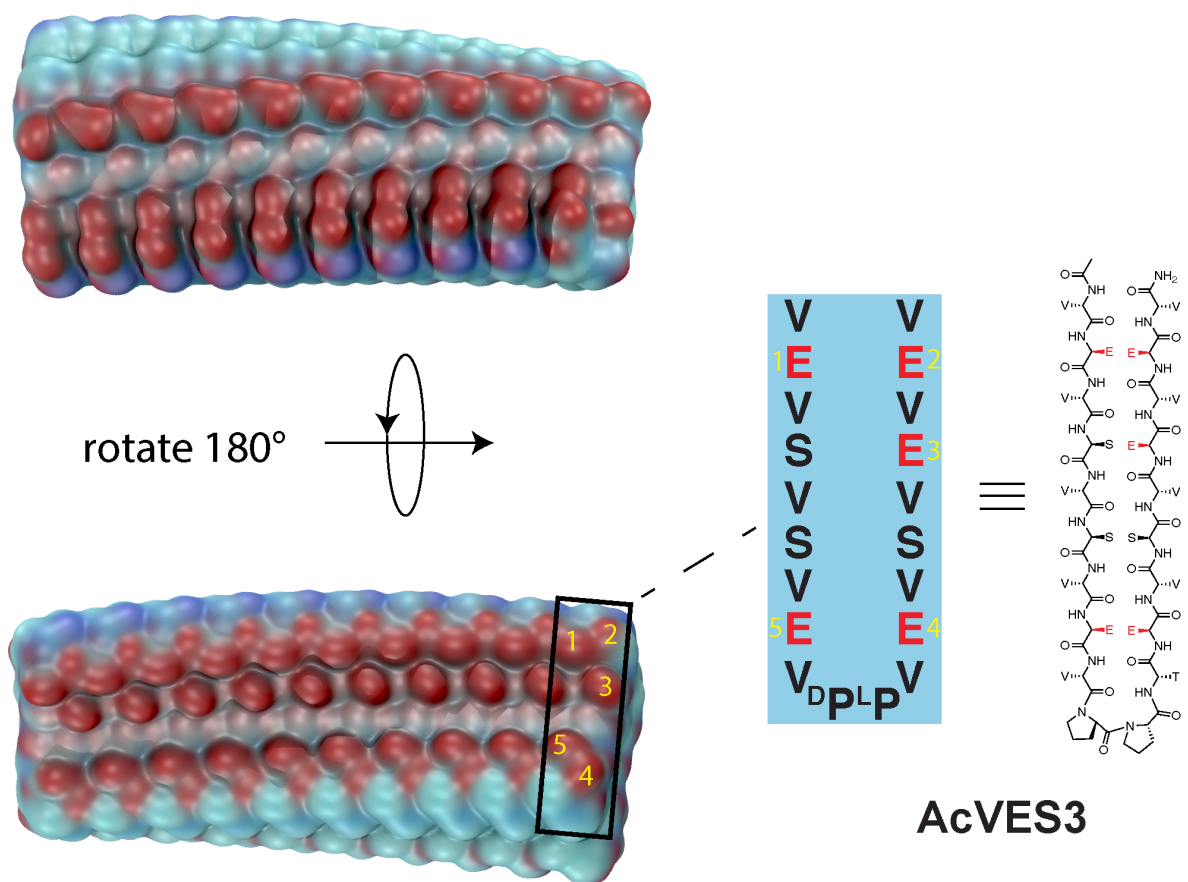


Figure S13. Model of the AcVES3 fiber used for MD simulations. The assembly of the peptide results in the display of two hydrophilic faces within a given fiber, both of which contain strips of negative charge that traverse the fibril.

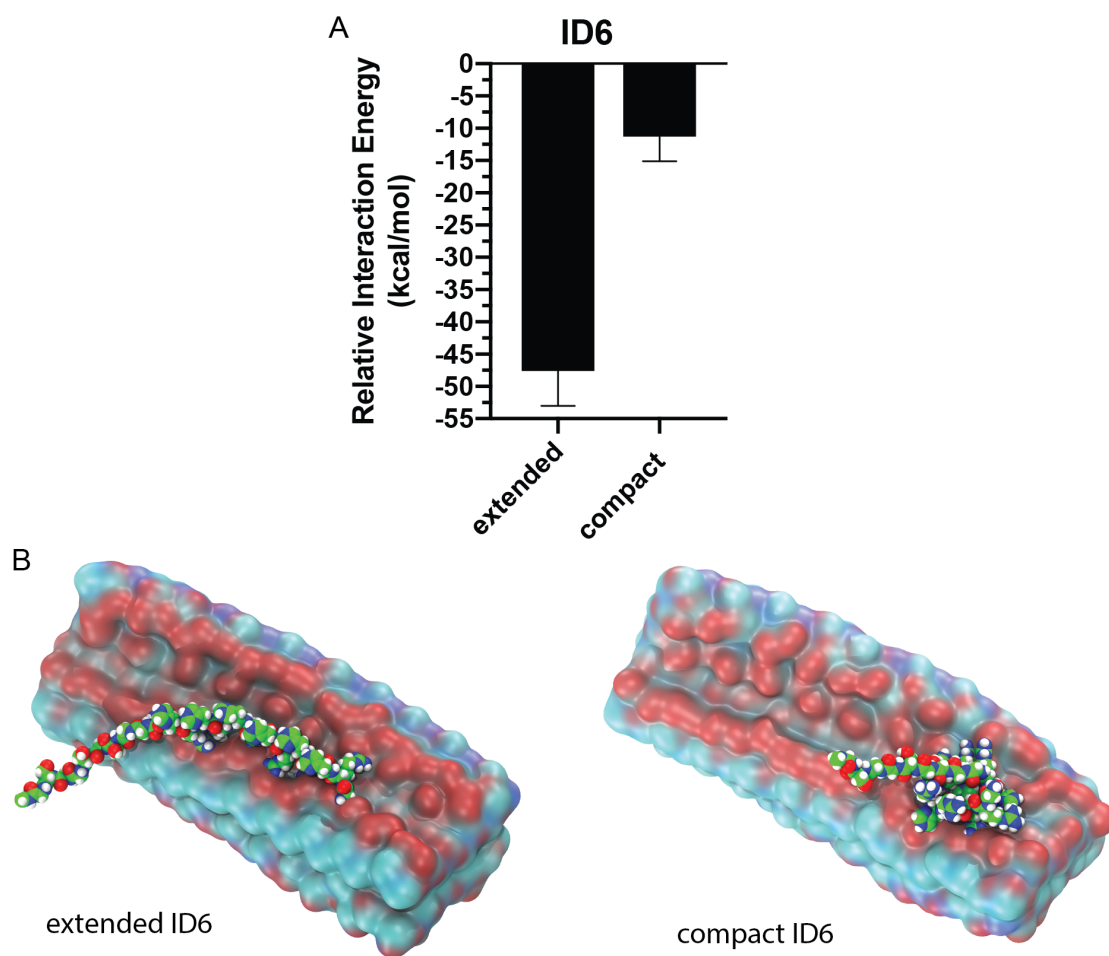


Figure S14. Assessing the preferred binding geometry of ID6. During initial MD simulations and docking, all IDs preferred to bind with the AcVES3 fiber in an extended conformation. We then conducted additional simulations/docking where ID6 was forced into a compact state. A) The calculated interaction energy for the compact form of ID6 was substantially less favorable than the extended form. B) Visual representations of the docked poses of ID6 in the extended and compact states.

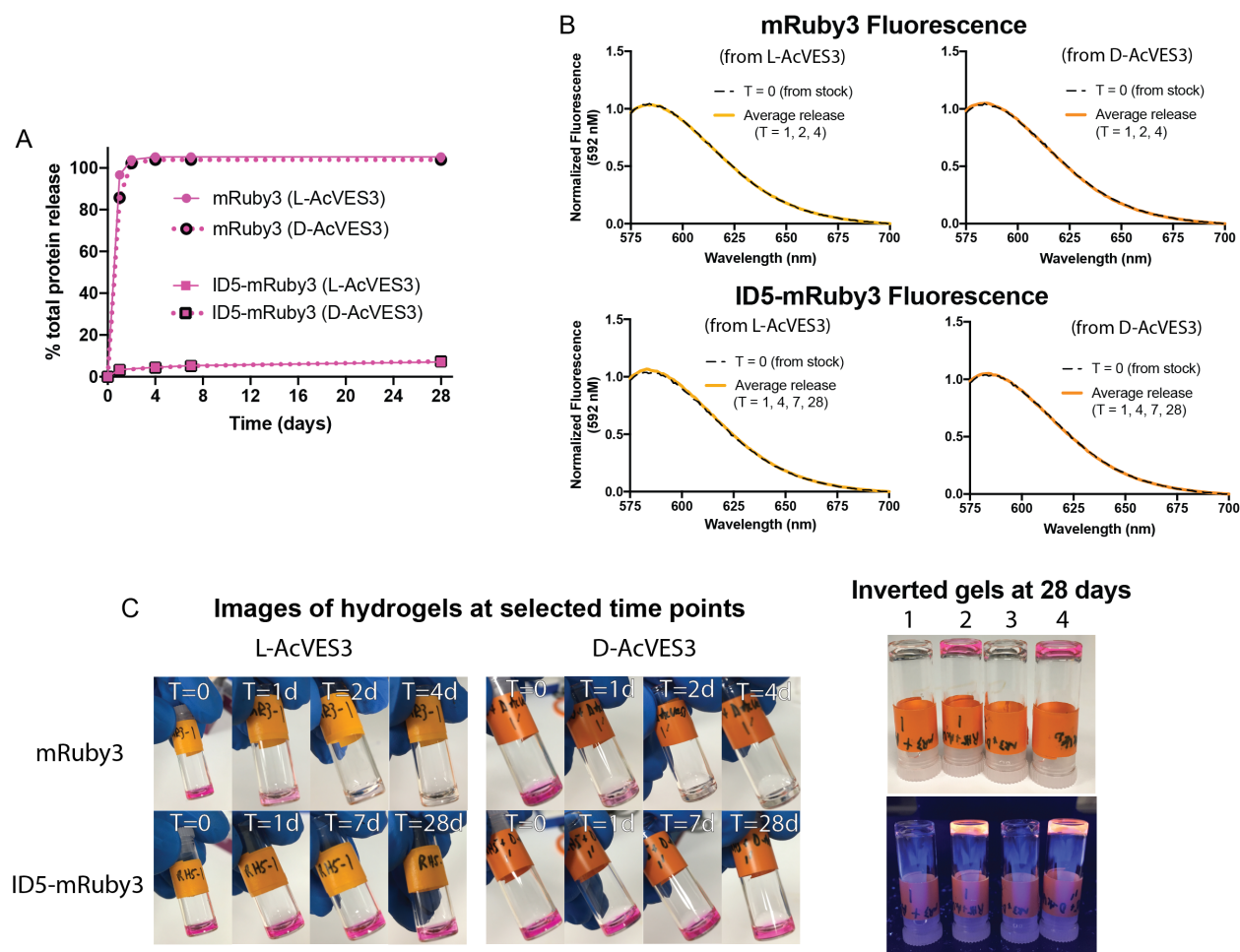


Figure S15. In vitro analysis of mRuby3 and ID5-mRuby3 release from AcVES3 hydrogels. A) Release from L-AcVES3 or D-AcVES3 were identical, indicating that the interaction between the cationic ID and the anionic peptide fibers is not inherently dependent on stereochemistry, but rather the general arrangement of charge on the surface of the fiber and within the ID. B) Normalized fluorescence spectra of mRuby3 analogs (592 nm), which shows that the protein remains active once released from the hydrogel. C) Images of protein loaded hydrogels at selected time points, demonstrating that the ID5-mRuby3-loaded gels retain fluorescence activity over the course of the in vitro study. On the right side of (C), 1) mRuby3 in L-AcVES3; 2) ID5-mRuby3 in L-AcVES3; 3) mRuby3 in D-AcVES3; 4) ID5-mRuby3 in D-AcVES3.

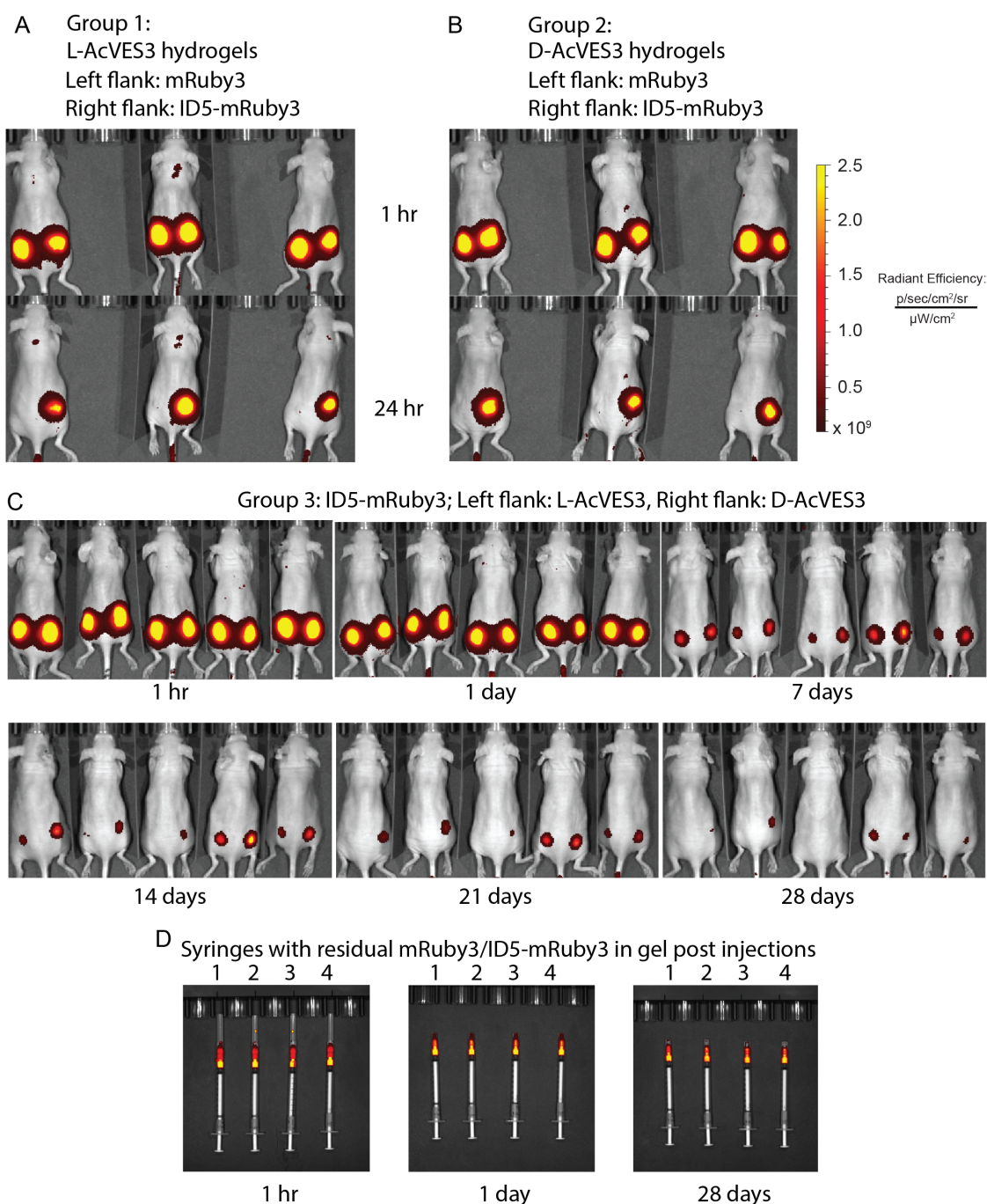


Figure S16. In vivo fluorescent images for mRuby3/ID5-mRuby3 release from AcVES3 hydrogels at selected time points. For both L-AcVES3 (A) and D-AcVES3 (B) hydrogels, mRuby3 was rapidly released within a day, while ID5-mRuby3 injection sites had a robust fluorescent signal indicating the retainment of protein. C) Prolonged release experiments comparing side-by-side release of ID5-mRuby3 from either L- or D-AcVES3 hydrogels. D-AcVES3 generally retained the protein for a longer period, with most mice having detectable levels after a month. D) Syringes with residual protein/gel were imaged at the same intervals and retained strong fluorescence throughout the study, with no significant photobleaching. Syringe 1: mRuby3 + L-AcVES3; Syringe 2: ID5-mRuby3 + L-AcVES3; Syringe 3: mRuby3 + D-AcVES3; Syringe 4: ID5-mRuby3 + D-AcVES3.

Table S1. Parameters used in molecular dynamics simulations. Molecular modeling codes used: Amber16, Xplor-NIH, GAMYR v3.0, FRMD, VMD, ZDOCK, ZRANK. Molecular dynamics simulations performed using GPU accelerated Amber16.²

Force Field:	ff14SB
Water model:	SPC
Periodic Box Cushion:	15 Å (free IDs); 18 Å (fibers/complexes)
Approximate # of water molecules:	~15,000 (free IDs); ~35,000 (fibers)
Salt (NaCl) concentration:	150 mM
Integration step:	0.002 ps
Restraints:	2.0 kcal/mol-Å ²
Production simulation time per model:	> 200 ns per model
Equilibration time:	5 ns
Trajectory update frequency:	20 ps
Temperature:	298.15 K
Barostat (isotropic, Berendsen) relaxation time:	0.5 ps
Thermostat Langevin collision frequency:	2.0/ps
Shake on bonds with H	

Supporting References

1. Kuruganti, S.; Accavitti-Loper, M. A.; Walter, M. R., Production and characterization of thirteen human type-I interferon- α subtypes. *Protein Expr. Purif.* **2014**, *103*, 75-83.
2. Case, D. A.; Betz, R. M.; Cerutti, D. S.; Cheatham III, T. E.; Darden, T. A.; Duke, R. E.; Giese, T. J.; Gohlke, H.; Goetz, A. W.; Homeyer, N.; Izadi, S.; Janowski, P.; Kaus, J.; Kovalenko, A.; Lee, T. S.; LeGrand, S.; Li, P.; Lin, C.; Luchko, T.; Luo, R.; Madej, B.; Mermelstein, D.; Merz, K. M.; Monard, G.; Nguyen, H.; Nguyen, H. T.; Omelyan, I.; Onufriev, A.; Roe, D. R.; Roitberg, A.; Sagui, C.; Simmerling, C. L.; Botello-Smith, W. M.; Swails, J.; Walker, R. C.; Wang, J.; Wolf, R. M.; Wu, X.; Xiao, L.; Kollman, P. A. *AMBER 2016*, University of California, San Francisco: 2016.
3. Nagy-Smith, K.; Moore, E.; Schneider, J.; Tycko, R., Molecular structure of monomorphic peptide fibrils within a kinetically trapped hydrogel network. *Proc. Natl. Acad. Sci. U.S.A.* **2015**, *112* (32), 9816-21.
4. Schwieters, C. D.; Kuszewski, J. J.; Clore, G. M., Using Xplor-NIH for NMR molecular structure determination. *Prog. Nucl. Mag. Res. Sp.* **2006**, *48* (1), 47-62.
5. Humphrey, W.; Dalke, A.; Schulten, K., VMD: visual molecular dynamics. *J. Mol. Graph. Model.* **1996**, *14* (1), 33-8, 27-8.
6. Bissantz, C.; Folkers, G.; Rognan, D., Protein-based virtual screening of chemical databases. 1. Evaluation of different docking/scoring combinations. *J. Med. Chem.* **2000**, *43* (25), 4759-4767.
7. Aqvist, J.; Medina, C.; Samuelsson, J. E., A new method for predicting binding affinity in computer-aided drug design. *Protein Eng.* **1994**, *7* (3), 385-91.
8. Brune, D.; Kim, S., Predicting protein diffusion coefficients. *Proc. Natl. Acad. Sci. U.S.A.* **1993**, *90* (9), 3835-9.
9. Hou, T.; Wang, J.; Li, Y.; Wang, W., Assessing the Performance of the MM/PBSA and MM/GBSA Methods. 1. The Accuracy of Binding Free Energy Calculations Based on Molecular Dynamics Simulations. *J. Chem. Inf. Model.* **2011**, *51* (1), 69-82.

10. Kastritis, P. L.; Rodrigues, J. P.; Folkers, G. E.; Boelens, R.; Bonvin, A. M., Proteins feel more than they see: fine-tuning of binding affinity by properties of the non-interacting surface. *J. Mol. Biol.* **2014**, *426* (14), 2632-52.
11. Bidacovich, E. A.; Kalko, S. G.; Cachau, R. E., Gamyr - a Generalized Version of Amyr for the Study of Biomolecules. *THEOCHEM* **1990**, *69*, 455-465.
12. Panel, N.; Sun, Y. J.; Fuentes, E. J.; Simonson, T., A Simple PB/LIE Free Energy Function Accurately Predicts the Peptide Binding Specificity of the Tiam1 PDZ Domain. *Front. Mol. Biosci.* **2017**, *4* (65), 65.
13. Hawkins, G. D.; Cramer, C. J.; Truhlar, D. G., Pairwise Solute Descreening of Solute Charges from a Dielectric Medium. *Chem. Phys. Lett.* **1995**, *246* (1-2), 122-129.
14. Zhou, R. H.; Friesner, R. A.; Ghosh, A.; Rizzo, R. C.; Jorgensen, W. L.; Levy, R. M., New linear interaction method for binding affinity calculations using a continuum solvent model. *J. Phys. Chem. B* **2001**, *105* (42), 10388-10397.
15. Tounge, B. A.; Reynolds, C. H., Calculation of the binding affinity of beta-secretase inhibitors using the linear interaction energy method. *J. Med. Chem.* **2003**, *46* (11), 2074-82.
16. Huang, D.; Caflisch, A., Efficient evaluation of binding free energy using continuum electrostatics solvation. *J. Med. Chem.* **2004**, *47* (23), 5791-5797.
17. Singh, N.; Warshel, A., Absolute binding free energy calculations: On the accuracy of computational scoring of protein-ligand interactions. *Proteins* **2010**, *78* (7), 1705-1723.
18. Kolb, P.; Huang, D.; Dey, F.; Caflisch, A., Discovery of Kinase Inhibitors by High-Throughput Docking and Scoring Based on a Transferable Linear Interaction Energy Model. *J. Med. Chem.* **2008**, *51* (5), 1179-1188.
19. Petrauskas, V.; Maximowitsch, E.; Matulis, D., Thermodynamics of Ion Pair Formations Between Charged Poly(Amino Acid)s. *J. Phys. Chem. B* **2015**, *119* (37), 12164-12171.